Ergodic Capacity and Error Performance of Spatial Diversity UWOC Systems over Generalized Gamma Turbulence Channels

Hongyan Jiang [1,2], Hongbing Qiu [1], Ning He [1,2], Wasiu Popoola [3], *Senior Member, IEEE*, Zahir Ahmad [4], and Sujan Rajbhandari [5,*], *Senior Member, IEEE*

[1] School of Information and Communication, Guilin University of Electronic Technology, Guilin 541004, China; qiuhb@guet.edu.cn, eicnhe@guet.edu.cn

[2] Guangxi Key Laboratory of Wireless Broadband communication and Signal Processing, Guilin 541004, China; jianghy@guet.edu.cn

[3] School of Engineering, Institute for Digital Communications, University of Edinburgh, Edinburgh EH8 9YL, UK; w.popoola@ed.ac.uk

[4] School of Computing, Electronics and Mathematics, Coventry University, Coventry CV1 5FB, UK; ab7175@coventry.ac.uk

[5] School of Computer Science and Electronic Engineering, Bangor University, Bangor, LL57 1UT, UK; s.rajbhandari@bangor.ac.uk;

* Correspondence: sujan@ieee.org

Abstract: In this paper, we study the ergodic capacity (EC) and average bit error rate (BER) of spatial diversity underwater wireless optical communications (UWOC) over the generalized gamma (GG) fading channels using quadrature amplitude modulation (QAM) direct current-biased optical orthogonal frequency division multiplexing (DCO-OFDM). We derive closed-form expressions of the EC and BER for the spatial diversity UWOC with the equal gain combining (EGC) at receivers based on the approximation of the sum of independent identical distributed (i.i.d) GG random variables (RVs). Numerical results of EC and BER for QAM DCO-OFDM spatial diversity systems over GG fading channels are presented. The numerical results are shown to be closely matched by the Monte Carlo simulations, verifying the analysis. The study clearly shows the adverse effect of turbulence on the EC & BER and advantage of EGC to overcome the turbulence effect.

Keywords: average bit error rate; ergodic capacity; generalized gamma; underwater wireless optical communications; spatial diversity; OFDM

1. Introduction

Underwater wireless optical communication (UWOC) is considered as an attractive complementary solution to underwater acoustic communication due to its high data rate, low latency and low implementation cost [1]. However, there are several challenges in implementing the UWOC system due to the adverse channel condition caused by absorption, scattering and turbulence in the oceanic environment [2]. There have been several attempts to establish a realistic channel model that can accurately predict the performance of the UWOC [1]-[9]. The attenuation due to absorption and scattering is well understood and mostly modelled by the radiative transfer equation [3], ray-tracing simulations [4], and a closed-form expression by fitting simulation data [5]. Underwater optical turbulence (UOT) caused by the variations in the refractive index due to temperature fluctuation, salinity variations and the presence of air bubbles adversely affect the link performance [6]-[7]. Hence, there has been significant attention to accurately characterize the UWOC turbulence channel to predict the performance and establish mitigation techniques [8]-[9].

The early studies on the UOT channel adopted lognormal distribution which is commonly used to describe atmospheric turbulence in free-space optical (FSO) system. However, the mechanisms of

turbulence generation in underwater and FSO channels are different and hence the lognormal distribution does not accurately model the UOT in all the conditions [7]. Subsequently, several studies of UOT have been carried out taking into account of several fading causes. In [10], a generalized gamma distribution was proposed to describe the temperature-induced weak turbulence. In [11], it was verified that Weibull distribution matches the measured data under all turbulence channels caused by salinity gradient. However, it was shown in [12] that the measured data in the presence of air bubbles do not fit well by a single-lobe distribution and required a two-lobe statistical model. Taking into account both air bubbles and temperature gradient, an exponential-generalized gamma (EGG) distribution model was proposed in [7] which excellently matches the experimental data under all channel conditions. Using beam expander-and-collimator (BEC) at the transmitter side and/or aperture averaging lens (AAL) at the receiver side, it was shown in [13] that the GG and exponential Weibull distributions provide an excellent agreement with the measured data in UWOC channels with random temperature and salinity variations in the presence of air bubbles, covering a wide range of scintillation index values from weak to strong turbulence. In fact, GG distribution is a general case of some of the important statistical distributions in modelling fading such as exponential, Rayleigh, gamma, Weibull, Nakagami-*m* and lognormal [13]-[14].

It was established that turbulence-induced fading considerably increases the average bit error rate (BER) and hence results in a large power penalty to achieve desired BER performance. This, in turn, either significantly reduces the communication range or decreases the maximum achievable data rate. To mitigate fading impairments, several techniques have been proposed, including a) error control coding in conjunction with interleaving [15]-[16], b) maximum likelihood sequence detection [17], c) multi-hop relaying transmission [18] and d) spatial diversity[19][20]. The first three approaches have several practical limitations, namely large-size interleaves, high computational complexity and high cost, but spatial diversity is not only the most practical and effective to mitigate the fading but also reduces the possibility of temporal blockage by multiple apertures at the transmitter and/or the receiver[21]. The spatial diversity scheme involves repetition coding at the transmitter and linear diversity combining (LDC) technique at the receiver. There are three well-known LDC techniques, namely maximal ratio combining (MRC), equal gain combining (EGC) and selection combining (SC). Though MRC offers the best performance, it requires prior channel knowledge which is very difficult to obtain especially for a time-varying channel[21]. Furthermore, the performance of EGC can match very close to MRC for most practical cases [22]. Therefore, EGC is a more realistic option for practical implementation due to its simplicity and low complexity [23].

The selection of the modulation scheme also affects the performance of UWOC in the oceanic turbulence channel. The intensity modulation and direct detection with baseband modulation such as On-Off keying (OOK) and pulse position modulation (PPM) are frequently used for UVLC due to their simplicity and low cost. Though simple to implement, OOK needs adaptive detection to achieve optimal performance in UOT channel [24]. PPM scheme, on the other hand, requires a very tight pulse and symbol synchronization and has inferior bandwidth efficiency compared to OOK. The subcarrier modulation (SCM) scheme is an alternative to the baseband modulation[25]. The SCM permits the use of high-order constellations such as *M*-ary phase-shift keying (*M*-PSK) and *M*-QAM by modulating an RF signal onto the intensity of the optical beam [26]. The OFDM is a special case of SCM, where the carriers are orthogonal over one symbol period. OFDM offers high spectral efficiency, resistance to inter-symbol interference and frequency selective fading[27][28].To meet the real and unipolar requirement of optical intensity modulation, several modified OFDMs were proposed, such as DCO-OFDM, asymmetrically-clipped optical OFDM (ACO-OFDM), and asymmetrically clipped DC-biased Optical OFDM (ADO-OFDM). DCO-OFDM is usually adopted in high bit rate communication due to its high bandwidth utilization.

Although GG distribution has been shown to adequately model fading channels, there are very limited studies to evaluate the performance of various spatial diversity schemes over GG fading channels. Aalo *et al* derived the average symbol error rate performance of multilevel modulation

schemes for wireless communication systems in GG channels with diversity receivers [29]. Sagias *et al* derived and evaluated union upper bounds for the outage and the average bit error probability for ECG receivers[30]. In addition, Costa in [31] used another GG RV to approximate the sum of independent identical distributed (i.i.d) GG RVs) and then derived the analytical expressions of outage probability and average BER for the spatial-diversity wireless communication systems using noncoherent frequency shift keying and noncoherent differential phase-shift keying. However, to the best knowledge of the authors, there is no prior work to evaluate the ergodic capacity and average BER of QAM-OFDM for spatial diversity UWOC systems over GG fading channels. Hence, in this paper, we propose and study DCO-OFDM with a diversity scheme and EGC reception to mitigate the fading and achieve high spectral efficiency. We derive a closed-form expression of average BER based on the approximation of the sum of GG RVs and Gauss-Laguerre quadrature integrals. We also derive the EC in terms of Fox's functions. Numerical results for average BER and EC of QAM DCO-OFDM with spatial diversity in the UWOC systems over GG fading channels are presented. The results are further validated by Monte-Carlo (MC) simulations. To the best of our knowledge, this is the first study of comprehensive mathematical derivation of the average BER and EC for DCO-OFDM under turbulent UWOC.

The rest of the paper is organized as follows: Section II describes the UWOC channel in the presence of UOT and DCO-OFDM with EGC diversity systems. In Section III, we derive the average BER and EC. In Section IV, numerical and simulation results are presented, compared and discussed. Finally, Section V concludes this paper.

2. UWOC system and channel model

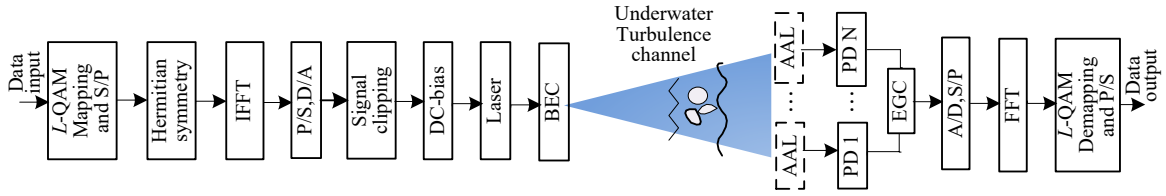

Fig.1. The block diagram of the DCO-OFDM with diversity scheme for UWOC systems.

A block diagram of the proposed spatial diversity UWOC systems with DCO-OFDM scheme is shown in Fig. 1. We consider one transmitter and N receiving apertures (the total area is the same regardless of N) and standard modulation/ demodulation procedure of DCO-OFDM as described in [32]. The information bits are modulated employing L-QAM scheme (where $\log2(L)$ >0 is an integer), followed by a serial to parallel (S/P) converter. Before the inverse fast Fourier transform (IFFT) operation, Hermitian symmetry is imposed on the OFDM symbol to generate a real-valued signal. The outputs of IFFT operation are then serialized using parallel-to-serial (P/S) converter, followed by conversion to analogue signals using a digital-to-analogue converter (DAC) and a filter. The real signal is further converted to a unipolar signal to drive a linear optical modulator by clipping and direct current (DC)-bias addition. The DC-bias level I_{DC} is given as **Error! Reference source not found.**:

$$I_{DC} = g\sqrt{E_s}\ , \tag{1}$$

where g is the normalized bias and E_s is the energy per symbol. The signal is pre-clipped at $\pm I_{DC}$ to ensure a positive signal after addition of DC-bias [1].

Furthermore, the modulated beam is expanded and collimated to ease alignment. After propagating through the turbulence UWOC channel, the optical signal is received by photodetectors which can be equipped with AALs. EGC is adopted for the diversity scheme, and thus the total received instantaneous electrical signal is expressed as [17]:

$$y_{EGC}(t) = \sum_{i=1}^{N} y_i(t) = \eta I x(t) \sum_{i=1}^{N} \alpha_i h_i + n(t), \tag{2}$$

where η denotes the photodetector responsivity, $x(t)$ represents the OFDM signal, I is the irradiance, h is the path loss coefficient in the absence of fading, α is the fading coefficient, and the subscript i represents the ith branch. $n(t)$ is the additive white Gaussian noise (AWGN) with single-sided power spectral density N_0. We assume the path loss and fading are independent, and i.i.d fading at receiver apertures because their separation (generally on the order of centimeters) is sufficiently larger than coherence length (generally on the order of millimeters [34]), but not very far from each other.

The UOT is modelled as a GG statistical distribution such that the fading coefficient α_i has the probability density function (pdf) given by [14]:

$$f_{\alpha_i}(\alpha) = \frac{2v_i}{\left(\frac{\Omega_i}{m_i}\right)^{m_i} \Gamma(m_i)} \alpha^{2v_i m_i - 1} \exp\left(-\frac{m_i \alpha^{2v_i}}{\Omega_i}\right), \quad \alpha > 0 \tag{3}$$

where m_i, Ω_i and v_i are the fading, scaling and shape parameters, respectively, and $\Gamma(\cdot)$ represents the gamma function. The GG-distributed RV α_i is denoted as $\alpha_i \sim \mathrm{GG}(m_i, v_i, \Omega_i)$. Other statistical distributions that describe UOT such as gamma $(v_i = 0.5)$ [10], Weibull $(m_i = 1)$ [11], exponential $(v_i = 0.5, m_i = 1)$ [35] and lognormal $(m_i \to \infty, v_i \to 0)$ [2] are special or limiting cases of the GG distribution [13].

The nth moment of the GG-distributed fading coefficient α_i is given by:

$$\mathrm{E}[\alpha_i^n] = \left(\frac{\Omega_i}{m_i}\right)^{\frac{n}{2v_i}} \frac{\Gamma\left(m_i + \frac{n}{2v_i}\right)}{\Gamma(m_i)} \tag{4}$$

where $\mathrm{E}[\cdot]$ stands for the expectation operator. Thus, the scintillation index σ_I^2 can be expressed as [13]:

$$\sigma_I^2 = \frac{\mathrm{E}[\alpha_i^2] - \mathrm{E}^2[\alpha_i]}{\mathrm{E}^2[\alpha_i]} = \frac{\Gamma(m_i)\Gamma\left(m_i + \frac{1}{v_i}\right)}{\Gamma^2\left(m_i + \frac{1}{2v_i}\right)} - 1 \tag{5}$$

To ensure that no energy loss or gain occurs during the turbulence-induced fading process, the fading coefficient is normalized (i.e.,$\mathrm{E}[\alpha_i] = 1$).

The optical intensity fluctuation due to UOT is characterized by the multiplicative fading coefficient as shown in (2), whose corresponding electrical signal-to-noise ratio (SNR) is given by [24][25]:

$$\gamma_{EGC} = \frac{(\eta I)^2 \mathrm{E}[x^2(t)](\sum_{i=1}^{N} \alpha_i h_i)^2}{N_0} = \bar{\gamma}\left(\sum_{i=1}^{N} \alpha_i h_i'\right)^2 \tag{6}$$

where

$$\bar{\gamma} = \frac{(\eta I)^2 \mathrm{E}[x^2(t)]}{N_0}\left(\sum_{i=1}^{N} h_i\right)^2, \tag{7}$$

and

$$h_i' = \frac{h_i}{\sum_{i=1}^{N} h_i}, \tag{8}$$

where $\bar{\gamma}$ denotes the average SNR per QAM symbol in DCO-OFDM without turbulence, h_i' is the normalized path loss. When the DC-bias is large enough to avoid any clipping distortion, the effective SNR per received QAM symbol is given by[36]:

$$\gamma_{EGC}^{eff} = \frac{1}{1+g^2}\gamma_{EGC} = \frac{\bar{\gamma}}{1+g^2}\left(\sum_{i=1}^{N} \alpha_i h_i'\right)^2, \tag{9}$$

Assume $S = \sum_{i=1}^{N} \alpha_i h_i' = \sum_{i=1}^{N} \alpha_i'$ ($\alpha_i' \sim \mathrm{GG}(m_i, v_i, h_i'^{2v_i}\Omega_i)$) denotes the weighted sum, and then the γ_{EGC}^{eff} is written as

$$\gamma_{EGC}^{eff} = \frac{\bar{\gamma}}{1+g^2} S^2. \tag{10}$$

3. Performance analysis

To obtain the pdf of γ_{EGC}^{eff}, the pdf of the weighted sum should be evaluated. Another GG variable has been proposed to approximate the sum of multiple GG RVs. Thus, based on the pdf of the EGC output SNR, analytical expressions for average BER and EC with the EGC diversity scheme over the GG fading channels can be derived which are presented in forms of Fox's H-function.

A. The Parameters of the approximating GG RV

The GG-distributed weighted sum is denoted as $S \sim \mathrm{GG}(m, v, \Omega)$, and h_i is normalized to unity for simplicity. Based on the moment estimation, the parameters of S can be obtained by solving the following nonlinear equations [31]:

$$\frac{\Gamma^2\left(m+\frac{1}{2v}\right)}{\Gamma(m)\Gamma\left(m+\frac{1}{v}\right)-\Gamma^2\left(m+\frac{1}{2v}\right)} = \frac{\mathrm{E}^2(S)}{\mathrm{E}(S^2)-\mathrm{E}^2(S)}, \tag{11}$$

$$\frac{\Gamma^2\left(m+\frac{1}{v}\right)}{\Gamma(m)\Gamma\left(m+\frac{2}{v}\right)-\Gamma^2\left(m+\frac{1}{v}\right)} = \frac{\mathrm{E}^2(S^2)}{\mathrm{E}(S^4)-\mathrm{E}^2(S^2)}, \tag{12}$$

$$\Omega = m\left(\frac{\Gamma(m)\mathrm{E}(S)}{\Gamma\left(m+\frac{1}{2v}\right)}\right)^{2v}, \tag{13}$$

where the *n*-th moment of S can be derived from the individual moments of the GG summands as [31]:

$$\mathrm{E}(S^n) = \sum_{n_1=0}^{n}\sum_{n_2=0}^{n_1}\cdots\sum_{n_{N-1}=0}^{n_{N-2}} \binom{n}{n_1}\binom{n_1}{n_2}\cdots\binom{n_{N-2}}{n_{N-1}} \mathrm{E}\left(\alpha_1'^{\,n-n_1}\right)\mathrm{E}\left(\alpha_2'^{\,n_1-n_2}\right)\cdots\mathrm{E}\left(\alpha_N'^{\,n_{N-1}}\right). \tag{14}$$

With the aid of MATHEMATICA or similar tools, the parameters of S can be calculated.

B. The average symbol error rate

Using (9), the approximated conditional bit error probability of *L*-QAM is given by [37]:

$$p_e = \frac{4\left(\sqrt{L}-1\right)}{\sqrt{L}\log_2(L)} Q\left(S\sqrt{\frac{3\bar{\gamma}}{(L-1)(1+g^2)}}\right) + \frac{4\left(\sqrt{L}-2\right)}{\sqrt{L}\log_2(L)} Q\left(3S\sqrt{\frac{3\bar{\gamma}}{(L-1)(1+g^2)}}\right), \tag{15}$$

where $Q(\cdot)$ is the Gaussian Q-function. In the fading channels, the average BER is expressed as:

$$P_e = \int_0^\infty f_{GG}(S) p_e(S)\, dS. \tag{16}$$

With integration by parts and considering practical scenarios, the average BER is simplified as [38]:

$$P_e = -\int_0^\infty F_{GG}(S)\, dp_e(S), \tag{17}$$

where the CDF of GG distribution $F_{GG}(S)$ is given by:

$$F_{GG}(S) = \frac{\Upsilon\left(m,\ \frac{m}{\Omega}S^{2v}\right)}{\Gamma(m)}, \tag{18}$$

and $\Upsilon(a,x)$is the lower incomplete gamma function [39].

According to the definition of Gaussian Q-function, the derivative of $p_e$can be expressed as

$$\begin{aligned} dp_e(S) = -\frac{dS}{\sqrt{2\pi}}\sqrt{\frac{3\bar{\gamma}}{(L-1)(1+g^2)}}\Bigg\{&\frac{4\left(\sqrt{L}-1\right)}{\sqrt{L}\log_2(L)}\exp\left[-\frac{3\bar{\gamma}S^2}{2(L-1)(1+g^2)}\right] \\ &+\frac{12\left(\sqrt{L}-2\right)}{\sqrt{L}\log_2(L)}\exp\left[-\frac{27\bar{\gamma}S^2}{2(L-1)(1+g^2)}\right]\Bigg\}. \end{aligned} \tag{19}$$

Substituting (18) and (19) to (17) and then using variable substitution and the Gauss-Laguerre Quadrature shown as [40]:

$$\int_0^\infty x^{-1/2}e^{-x}f(x)dx \cong \sum_{i=1}^{n} H_i f(x_i) \tag{20}$$

equation (17) can be approximated by:

$$\begin{aligned} P_e = \frac{1}{2\sqrt{\pi}\Gamma(m)}\sum_{i=1}^{n} H_i\Bigg[&\frac{4\left(\sqrt{L}-1\right)}{\sqrt{L}\log_2(L)}\Upsilon\left(m,\frac{m}{\Omega}\left(\sqrt{\frac{2x_i(L-1)(1+g^2)}{3\bar{\gamma}}}\right)^{2v}\right) \\ &+\frac{4\left(\sqrt{L}-2\right)}{\sqrt{L}\log_2(L)}\Upsilon\left(m,\frac{m}{\Omega}\left(\sqrt{\frac{2x_i(L-1)(1+g^2)}{27\bar{\gamma}}}\right)^{2v}\right)\Bigg], \end{aligned} \tag{21}$$

where $x_i$is the ith zero of the Laguerre polynomial $L_n^{-1/2}(x)$ and H_i is the corresponding weight coefficient detailed in [40].

C. Ergodic capacity

Using (10), the EC of the EGC diversity systems over fading channels in bps/Hz is given by:

$$\bar{C} = \frac{\mathrm{E}\left[\ln\left(1+\gamma_{EGC}^{eff}\right)\right]}{\ln 2} = \frac{1}{\ln 2}\mathrm{E}\left[\ln\left(1+\frac{\bar{\gamma}}{1+g^2}S^2\right)\right]. \tag{22}$$

Let $Z = S^2$, and thus Z satisfies $Z \sim \mathrm{GG}(m, v/2, \Omega)$. Then, (22) can be expressed as

$$\bar{C} = \frac{1}{\ln 2}\int_0^\infty \ln\left[1+\frac{\bar{\gamma}}{1+g^2}Z\right]\frac{v}{\Gamma(m)}\left(\frac{\Omega}{m}\right)^{-m} Z^{mv-1}\exp\left(-\frac{m}{\Omega}Z^v\right)dZ. \tag{23}$$

By substituting $Y = \left(\frac{m}{\Omega}\right)^{1/v} Z$ in (23), we have:

$$\bar{C} = \frac{1}{\ln 2}\int_0^{\infty} \ln\left[1 + \frac{\bar{\gamma}}{1+g^2}\left(\frac{m}{\Omega}\right)^{-1/v} Y\right] \frac{v}{\Gamma(m)} Y^{mv-1} \exp(-Y^v)\, dY. \tag{24}$$

To simplify (24) in the form of Fox's H function, firstly we express the logarithmic function in the forms of Meijer's G function given by [41]:

$$\ln(1+x) = G_{2,2}^{1,2}\left[x\middle|_{1,0}^{1,1}\right]. \tag{25}$$

Furthermore, using the transforms between Meijer's G function and Fox's H function given by [42]:

$$H_{p,q}^{e,f}\left[x\middle|\begin{matrix}(a_i,1)_{1,p}\\(b_i,1)_{1,q}\end{matrix}\right] = G_{p,q}^{e,f}\left[x\middle|\begin{matrix}(a_i)_{1,p}\\(b_i)_{1,q}\end{matrix}\right], \tag{26}$$

and then using the product of power and exponential functions expressed by [42]:

$$H_{0,1}^{1,0}\left[x\middle|\overline{(b,\beta)}\right] = \frac{1}{\beta} x^{b/\beta} \exp(-x^{\frac{1}{\beta}}), \tag{27}$$

equation (24) is written as:

$$\bar{C} = \frac{1}{ln\, 2\Gamma(m)} \int_0^{\infty} Y^{mv-v-1} H_{0,1}^{1,0}\left[\frac{\bar{\gamma}}{1+g^2}\left(\frac{m}{\Omega}\right)^{-1/v} Y\middle|\begin{matrix}(1,1),(1,1)\\(1,1),(0,1)\end{matrix}\right] H_{0,1}^{1,0}\left[Y\middle|\overline{(1,1/v)}\right] dY. \tag{28}$$

Finally, using integral formulas involving the H-function given by [42,2.8.4], we have:

$$\bar{C} = \frac{1}{\ln 2\, \Gamma(m)} H_{3,2}^{1,3}\left[\frac{\bar{\gamma}}{1+g^2}\left(\frac{m}{\Omega}\right)^{-1/v}\middle|\begin{matrix}(1,1),(1,1),(1-m,1/v)\\(1,1),(0,1)\end{matrix}\right]. \tag{29}$$

By using (29), we can evaluate the EC of the EGC diversity systems over GG fading channels.

4. Results and Discussion

In this section, numerical results for the average BER and EC based on the analytical expressions and MATHEMATICA are presented for different diversity orders under various GG fading conditions. To verify the analytical results, the results of the MC simulations, using MATLAB, are also presented. Based on the study in [13], two fading channel scenarios are considered and their corresponding parameters of GG RVs are shown in Table I.

Table I the parameters of i.i.d GG-distributed fading channels based on Table III and IV of [13]

Channel condition	m_i	v_i	Ω_i	σ_I^2
Salinity random variations	1.62	0.72	1.1	0.31
Temperature random variations mixed presence of air bubbles	1.4	0.42	0.94	1.02

Fig.2 depicts the pdf of the sum of four i.i.d GG-distributed RVs, i.e., for a diversity order of 4. The theoretical pdf is evaluated using (10) to (13), which is verified by Monte Carlo simulation. Four i.i.d GG-distributed RVs are generated based on the inverse transform method. Then, the histogram of their sum is obtained to compare with the theoretical pdf. Fig.2 clearly shows a good agreement between the theoretical and simulation results for $\sigma_I^2 = 0.31$ and 1.02, which is the basis for average BER and EC evaluation in the following section.

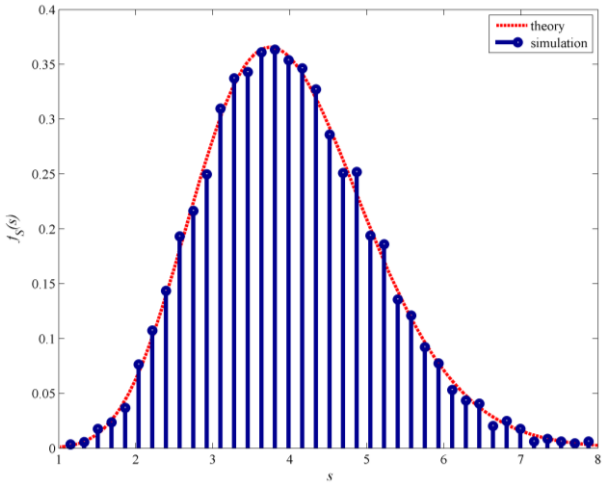

(a) $\sigma_I^2 = 0.31$

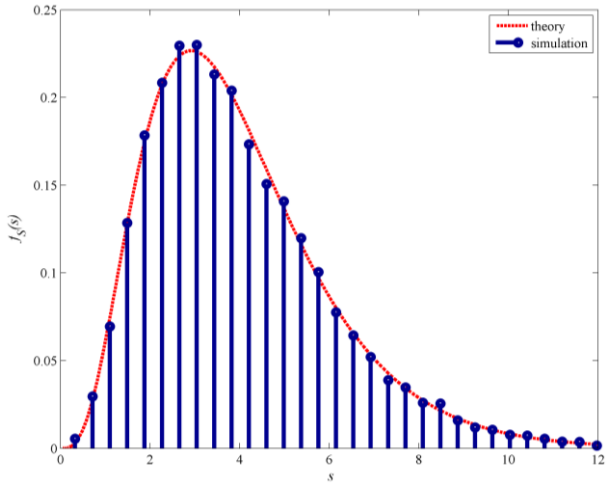

(b) $\sigma_I^2 = 1.02$

Fig. 2 The pdf of the sum of four GG RVs (i.e., $N = 4$).

Additionally, the MC simulation of QAM DCO-OFDM system has been validated by comparing the BERs in fading-free AWGN channel with results in [33]. For the simulation, we have taken the standard MC simulation approach of generating a pseudorandom binary sequence (PRBS) of 2^{19} bits, converting them to an OFDM signal and transmitting them through the fading-free AWGN channel. At the receiver, the OFDM decoding is achieved as shown in Fig. 1. Finally, the transmitted and received binary sequences are compared and BER is estimated. In Fig.3, the BER in AWGN versus average E_b/N_0 (i.e., SNR per bit) for the SISO QAM DCO-OFDM (N = 1) system is very close to the results provided in [33] obtained under the same simulation condition such as constellation size, DC-bias level and clipping level. Note that here the OFDM signal is only pre-clipped at a bottom level of $-I_{DC}$. This verifies the study in AWGN is valid. Moreover, the BER for the spatial diversity scheme with N = 4 and EGC is presented. The simulation results show that the diversity scheme and SISO scheme have the same BER in AWGN, i.e., no diversity gain was observed in the absence of turbulence-induced fading. Hence, the SNR gain in the turbulence channel is attributed to the diversity scheme used.

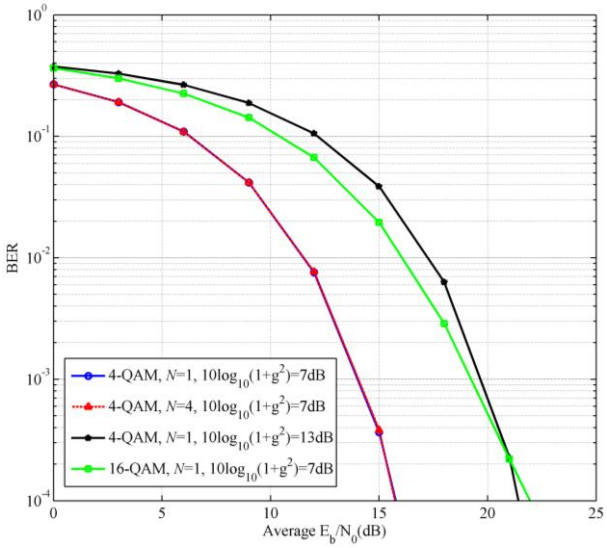

Fig.3 BERs versus average E_b/N_0 for 4 & 16-QAM DCO-OFDM scheme in AWGN based on MC simulation

Next, we analyzed and compared the BER performance of the diversity scheme with EGC over GG-distributed fading channels. The UOWC channel is slow fading and hence, a constant fading coefficient is considered over an OFDM symbol which changes with OFDM symbols [13]. The analytical and simulated average BERs versus average SNR per QAM symbol for the 4&16-QAM-OFDM scheme over GG fading channels with $\sigma_I^2 = 0.31$ and 1.02 are shown in Fig. 4, where the normalized bias is assumed as g = 3 to ensure no clipping distortion. It is observed that there is a close match between the analytical and simulated results in weak and strong turbulence channels, thereby validating the accuracy of approximated analytical expressions. The agreement between analytical and simulated BERs in the case of 4-QAM is better than that in the case of 16-QAM because the truncation error in (15) increases with increasing constellation size.

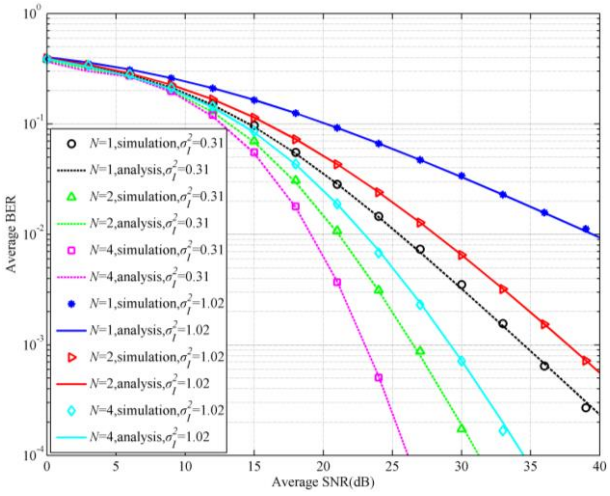

(a) 4-QAM

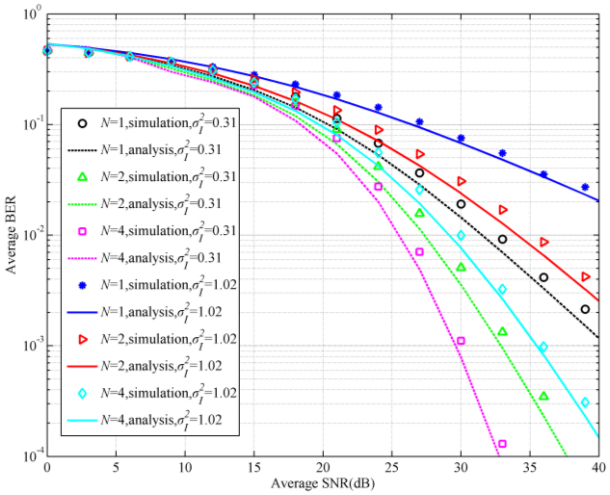

(b) 16-QAM

Fig.4 Average BERs versus the average SNR for 4 & 16-QAM DCO-OFDM scheme over GG UOWC fading channels.

Furthermore, in Fig. 4 it is clearly shown that the BER performance degrades with the increasing scintillation index, and spatial diversity can effectively mitigate the effect of turbulence. A large diversity gain can be obtained by increasing the diversity order. For example, seen from Fig.4(a), for a weak turbulence channel with $\sigma_I^2 = 0.31$, the diversity order of 2 requires ~3.5 dB higher SNR than that for diversity order of 4 to achieve a BER of 10^{-3}. For a strong turbulence channel with $\sigma_I^2 = 1.02$, the diversity gain difference increases to 8.5 dB. This clearly demonstrates the advantage of a large diversity order for strong turbulence channels. By comparing Fig.4(a) and (b), the trade-off between spectral efficiency and reliability is shown as that 16-QAM system requires higher SNR or larger diversity order than 4-QAM to achieve the same BER performance.

Fig.5 illustrates the analytical and simulated EC per unit bandwidth for no diversity and diversity orders of 2 and 4 over GG-distributed fading channel. In the simulation, 10^5 GG random samples are generated for each branch to evaluate the EC for receiver diversity with EGC. Fig.5 demonstrates that there is a good agreement between the simulation and analytical results, validating the analytical expression. Similar to BER, by comparing Fig.5(a) and (b), ECs decrease as the turbulence strength increases. Unlike the case of BER performance, the improvement in EC due to the diversity scheme is not obvious in a weak turbulence channel. The diversity gain of $N = 2$ and 4 is close, as the diversity gain saturates at a higher diversity order. However, with increasing the turbulence strength, spatial diversity is necessary to ensure a large EC, which can be seen from Fig.5. With the scintillation index changing from 0.31 to 1.02, ECs drop 0.8, 0.4 and 0.2 bps/Hz for the scheme of N=1, 2 and 4 at SNR = 30 dB, respectively, demonstrating the necessity of spatial diversity. Thus, the results are useful to practical system design in terms of the relation among average BER, EC, diversity order and SNR over various GG fading channels.

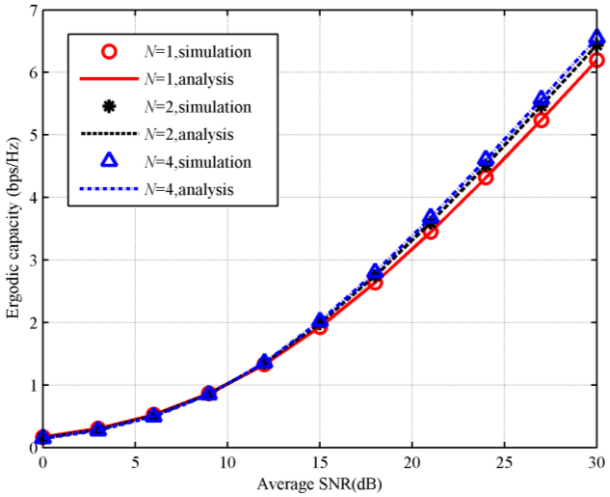

(a) $\sigma_I^2 = 0.31$

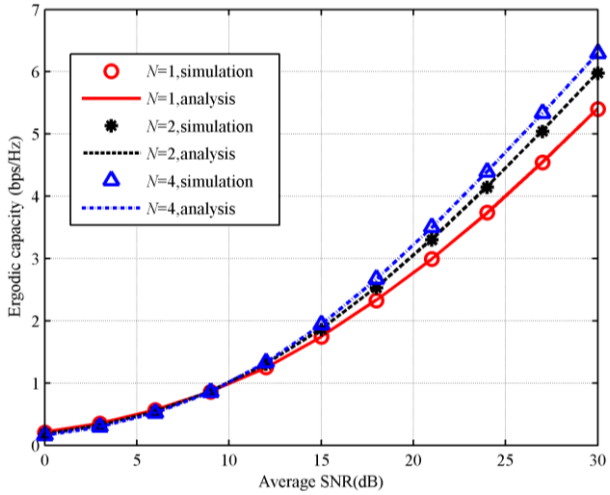

(b) $\sigma_I^2 = 1.02$

Fig.5 ECs versus average SNR in GG fading channels.

5. Conclusion

In this paper, the spatial diversity with EGC was proposed to combat turbulence-induced fading impairments in UWOC systems over GG channels. Based on the approximation of the sum of GG RVs, the average BER and EC for QAM-DCO-OFDM were evaluated. Using Gauss-Laguerre quadrature integral, a closed-form expression of the average BER is derived. In addition, with the help of transforms and integral formulas involving Fox's H function, the EC is given in the forms of Fox's H function. Based on the derived closed-form expressions, the analytical results of BERs for 4 & 16-QAM DCO-OFDM with diversity schemes over GG fading channels are calculated and compared with the Monte-Carlo simulation results. In addition, the analytical and simulated ECs per unit bandwidth are also presented. All the results showed excellent agreement between the analysis and simulation, validating the theoretical analysis. It is shown that increasing diversity order improves BER performance and EC, especially in strong turbulence. However, the gain saturates at higher diversity order. Meanwhile, cost and complexity increase with increasing diversity order. Hence, a careful trade-off is required to optimize the performance with a cost-effective solution. The obtained results are useful for designing, predicting and evaluating the DCO-OFDM spatial diversity UOWC system in various fading scenarios.

Author Contributions: Conceptualization, H.J. and S.R.; methodology, H.J. and S.R.; software, H.J. and S.R.; validation, H.J. and S.R.; investigation, H.J., S.R. and N.H.; writing—original draft preparation H.J. and S.R.;

writing—review and editing, S.R., W.P. and Z.A.; supervision, S.R. and H.Q.; funding acquisition, N.H. and H.J.. All authors have read and agreed to the published version of the manuscript.

Funding: This research was funded in part by the National Natural Science Foundation of China (grant number 61961008 and 61761014), in part by the Dean Project of Guangxi Key Laboratory of Wireless Broadband Communication and Signal Processing (grant number GXKL06200127), and in part by the project of improving basic ability of scientific research for middle-aged and young scholars of higher education of Guangxi (grant number 2020KY05028)

Conflicts of Interest: The authors declare no conflict of interest.

References

[1] L. Zhang, H. Wang, and X. Shao, "Improved m-QAM-OFDM transmission for underwater wireless optical communications," Opt. Commun., vol. 423, no. March, pp. 180–185, 2018.

[2] Jiang H , Qiu H , He N , et al., "Performance of spatial diversity DCO-OFDM in a weak turbulence underwater visible light communication channel," *J. Light. Technol.*vol. 38, no.8, pp. 2271-2277, Apr. 2020.

[3] C. Li, K.-H. Park, and M.-S. Alouini, "On the use of a direct radiative transfer equation solver for path loss calculation in underwater optical wireless channels," *IEEE Commun. Lett.,* vol. 4, no. 5, pp. 561–564, Oct. 2015.

[4] F. Miramirkhani and M. Uysal, "Visible light communication channel modeling for underwater environments with blocking and shadowing," *IEEE Access*, vol. 6, no. 1, pp. 1082–1090, Dec. 2017.

[5] C. Wang, H.-Y. Yu, and Y.-J. Zhu, ''A long distance underwater visible light communication system with single photon avalanche diode,'' *IEEE Photon. J.,* vol. 8, no. 5, Oct. 2016, Art. no. 7906311.

[6] T. V. Pham, T. C. Thang, and A. T. Pham, "Average Achievable Rate of Spatial Diversity MIMO-FSO Over Correlated Gamma–Gamma Fading Channels," *J. Opt. Commun. Netw.,* vol. 10, no. 8, p. 662, 2018.

[7] E. Zedini, H. M. Oubei, A. Kammoun, M. Hamdi, B. S. Ooi, and M. S. Alouini, "Unified Statistical Channel Model for Turbulence-Induced Fading in Underwater Wireless Optical Communication Systems," *IEEE Trans. Commun.*, vol. 67, no. 4, pp. 2893–2907, 2019.

[8] W. Wang, P. Wang, T. Cao, H. Tian, Y. Zhang, and L. Guo, "Performance investigation of underwater wireless optical communication system using M-ary OAMSK modulation over oceanic turbulence," *IEEE Photon. J.*, vol. 9, no. 5, pp. 1-15, Oct. 2017.

[9] C. T. Geldard, J. Thompson and W. O. Popoola, "Empirical Study of the Underwater Turbulence Effect on Non-Coherent Light," in IEEE Photonics Technology Letters, vol. 32, no. 20, pp. 1307-1310, 2020.

[10] H. M. Oubei et al., "Simple statistical channel model for weak temperature-induced turbulence in underwater wireless optical communication systems," *Opt. Lett.*, vol. 42, no. 13, pp. 2455–2458, 2017.

[11] H. M. Oubei et al., "Efficient Weibull channel model for salinity induced turbulent underwater wireless optical communications," *in Proc. Opto-Electron. Commun. Conf., Photon. Global Conf.*, Singapore, Aug. 2017, pp. 1-2.

[12] M. V. Jamali et al., "Statistical distribution of intensity fluctuations for underwater wireless optical channels in the presence of air bubbles," IWCIT 2016 - Iran Work. Commun. Inf. Theory, 2016.

[13] M. V. Jamali et al., "Statistical studies of fading in underwater wireless optical channels in the presence of air bubble, temperature, and salinity random variations," *IEEE Trans. Commun.*, vol. 66, no. 10, pp. 4706–4723, 2018.

[14] V. A. Aalo, T. Piboongungon, and C. D. Iskander, "Bit-error rate of binary digital modulation schemes in generalized gamma fading channels," *IEEE Commun. Lett.*, vol. 9, no. 2, pp. 139–141, 2005.

[15] M. Uysal, S. M. Navidpour, and J. T. Li, "Error rate performance of coded free-space optical links over strong turbulence channels," *IEEE Commun. Lett.*, vol. 8, no. 10, pp. 635-637, Oct. 2004.

[16] F. Mattoussi, M. A. Khalighi, and S. Bourennane, "Improving the performance of underwater wireless optical communication links by channel coding," Appl. Opt., vol. 57, no. 9, p. 2115-2120, 2018.

[17] M. V. Jamali, P. Nabavi, and J. A. Salehi, "MIMO underwater visible light communications: Comprehensive channel study, performance analysis, and multiple-symbol detection," *IEEE Trans. Veh. Technol.*, vol. 67, no. 9, pp. 8223–8237, 2018.

[18] M. V. Jamali, F. Akhoundi, and J. A. Salehi, "Performance Characterization of Relay-Assisted Wireless Optical CDMA Networks in Turbulent Underwater Channel," *IEEE Trans. Wirel. Commun.*, vol. 15, no. 6, pp. 4104–4116, Jun. 2016.

[19] A. Yilmaz, M. Elamassie, and M. Uysal, "Diversity gain analysis of underwater vertical MIMO VLC links in the presence of turbulence," *IEEE Int. Black Sea Conf. Commun. Networking*, BlackSeaCom 2019, pp. 1–6, 2019.

[20] R. ran Wang, P. Wang, T. Cao, L. Xin Guo, and Y. Yang, "Average bit error rate performance analysis of subcarrier intensity modulated MRC and EGC FSO systems with dual branches over M distribution turbulence channels," Optoelectron. Lett., vol. 11, no. 4, pp. 281–285, 2015.

[21] M. V. Jamali, J. A. Salehi, and F. Akhoundi, "Performance studies of underwater wireless optical communication systems with spatial diversity: MIMO scheme," *IEEE Trans. Commun.*, vol. 65, no. 3, pp. 1176–1192, Mar. 2017.

[22] M. Safari, S. Member, M. Uysal, S. Member, and I. M. Dd, "Do We Really Need OSTBCs for Free-Space Optical Communication with Direct Detection?" *IEEE Trans. Wirel. Commun.*, vol. 7, no. 11, pp. 4445–4448, 2008.

[23] V. K. Bhargava, "Equal-gain diversity receiver performance in wireless channels," *IEEE Trans. Commun.*, vol. 48, no. 10, pp. 1732–1745, 2000.

[24] W. O. Popoola and Z. Ghassemlooy, "BPSK subcarrier intensity modulated free-space optical communications in atmospheric turbulence," J. Light. Technol., vol. 27, no. 8, pp. 967–973, 2009.

[25] W.O. Popoola, Z. Ghassemlooy, J.I.H. Allen, E. Leitgeb, and S. Gao."Free-space optical communication employing subcarrier modulation and spatial diversity in atmospheric turbulence channel," IET Optoelectron. vol. 2, no. 1, pp. 16–23, 2008.

[26] M. R. Bhatnagar and Z. Ghassemlooy, "Performance Analysis of Gamma-Gamma Fading FSO MIMO Links with Pointing Errors," *J. Light. Technol.*, vol. 34, no. 9, pp. 2158–2169, 2016.

[27] A. Bekkali, C. Ben Naila, K. Kazaura, K. Wakamori, and M. Matsumoto, "Transmission analysis of OFDM-based wireless services over turbulent radio-on-FSO links modeled by gamma-gamma distribution," *IEEE Photonics J.*, vol. 2, no. 3, pp. 510–520, 2010.

[28] R. Hema, S. Sudha, and K. Aarthi, "Performance studies of MIMO based DCO-OFDM in underwater wireless optical communication systems," J. Mar. Sci. Technol., vol. 26, no. 1, pp. 97–107, 2021.

[29] V.A. Aalo, G.P. Efthymoglou, T. Piboongungon and C.D. Iskander, "Performance of diversity receivers in generalised gamma fading channels," *IET Commun.*, vol. 1, no. 3, pp. 341-347, 2007.

[30] N. C. Sagias, G. K. Karagiannidis, P. T. Mathiopoulos, and T. A. Tsiftsis, "On the performance analysis of equal-gain diversity receivers over generalized gamma fading channels," *IEEE Trans. Wirel. Commun.*, vol. 5, no. 10, pp. 2967–2975, 2006.

[31] D. B. Da Costa, M. D. Yazoub, and J. C. S. Santos Filho, "Highly accurate closed-form approximations to the sum of α-μ variates and applications," *IEEE Trans. Wirel. Commun.*, vol. 7, no. 9, pp. 3301–3306, 2008.

[32] S. Rajbhandari et al., "A review of gallium nitride LEDs for multi-gigabit-per-second visible light data communications," *Semicond. Sci. Technol.*, vol. 32, no. 2, pp. 023001 (1-40), 2017.

[33] J. Armstrong and B. J. C. Schmidt, "Comparison of asymmetrically clipped optical OFDM and DC-biased optical OFDM in AWGN," IEEE Commun. Lett., vol. 12, no. 5, pp. 343–345, 2008.

[34] L. Lu, X. Ji, and Y. Baykal, "Wave structure function and spatial coherence radius of plane and spherical waves propagating through oceanic turbulence," *Opt. Express*, vol. 22, no. 22, p. 27112, 2014.

[35] Z. Vali, A. Gholami, Z. Ghassemlooy, and D. G. Michelson, "System parameters effect on the turbulent underwater optical wireless communications link," Optik (Stuttg)., vol. 198, no. July, p. 163153, 2019.

[36] L. Chen, B. Krongold, and J. Evans, "Performance analysis for optical OFDM transmission in short-range IM/DD systems," *J. Light. Technol.,* vol. 30, no. 7, pp. 974–983, 2012.

[37] S. Dimitrov, S. Sinanovic, and H. Haas, "Clipping noise in OFDM-based optical wireless communication systems," IEEE Trans. Commun., vol. 60, no. 4, pp. 1072–1081, 2012.

[38] Y.T. Li, "Performance Analysis of the Channel Coding Technology of Underwater Wireless Optical Communication Systems based on Water Turbulence," *XiDian University*, Xi'an, China,2018.

[39] I. S. Gradshteyn and I. M. Ryzhik, Table of Integrals, Series, and Products (Seventh Edition). Academic Press, 2007.

[40] B. P. Conçus, D. Cassatt, G. Jaehnig, and E. Melby, "Tables for the Evaluation of $\int_0^\infty x^\beta e^{-x} f(x)dx$ by Gauss-Laguerre Quadrature," *Mathematics of Computation,* vol.17, no.83, pp.245-256, 1963.

[41] V. S. Adamchik and O. Marichev, "The algorithm for calculating integrals of hypergeometric type function and its realization in reduce system," in Proc. ISSAC, Tokyo, Japan, Aug. 1990, pp. 212–224.

[42] A.M. Mathai, R.K. Saxena and H.J. Haubold, "The H-Function, Theory and Applications", Springer, New York, 2010.